JOURNAL OF AIRCRAFT
Vol. 33, No. 2, March–April 1996

Flying-Qualities Analysis of an Unmanned Air Vehicle

R. M. Howard,* R. M. Bray,† and D. F. Lyons‡
U.S. Naval Postgraduate School, Monterey, California 93943

Flight tests of a half-scale radio-controlled model of the Pioneer unmanned air vehicle (UAV) were conducted for static longitudinal and lateral-directional stability-and-control characteristics. The air vehicle was instrumented to measure control-surface deflections, angle of attack, sideslip angle, and airspeed; telemetry was used to downlink the data to a ground recorder for later processing. A wind-tunnel test of a 0.4-scale Pioneer at full-scale Reynolds numbers was also carried out, as well as a numerical study using a low-order panel method. The flight-test determination of the neutral point agrees well with the other methods of prediction and indicated that the static margin was sufficient to open the restricted c.g. envelope. Other control-related considerations may provide overriding concerns, however. Crosswind limits were determined from steady-sideslip maneuvers and the flight data compared very favorably to that of the other data sources. Low-cost scaled-vehicle flight testing appears to be a viable tool in providing aerodynamic data for UAV simulation and training purposes.

Nomenclature

C_L = aircraft lift coefficient
$C_{L\alpha}$ = change in lift coefficient with change in angle of attack
$C_{L\delta e}$ = change in lift coefficient with elevator deflection
$C_{l\beta}$ = change in rolling moment coefficient with sideslip angle
$C_{l\delta a}$ = change in rolling moment coefficient with aileron deflection
$C_{l\delta r}$ = change in rolling moment coefficient with rudder deflection
$C_{m\alpha}$ = change in pitching moment with change in angle of attack
$C_{m\delta e}$ = change in pitching moment with elevator deflection
$C_{n\beta}$ = change in yawing moment coefficient with sideslip angle
$C_{n\delta a}$ = change in yawing moment coefficient with aileron deflection
$C_{n\delta r}$ = change in yawing moment coefficient with rudder deflection
$C_{Y\beta}$ = change in side force coefficient with sideslip angle
$C_{Y\delta a}$ = change in side force coefficient with aileron deflection
$C_{Y\delta r}$ = change in side force coefficient with rudder deflection
q = freestream dynamic pressure
α = angle of attack
β = sideslip angle
δ_a = aileron deflection
δ_e = elevator deflection
δ_r = rudder deflection
ϕ = bank angle

Presented in part as Papers 92-4075 and 92-4635 at the 6th Biennial Flight Test Conference, Hilton Head, SC, Aug. 24–26, 1992 and the AIAA Atmospheric Flight Mechanics Conference, Hilton Head, SC, Aug. 10–12, 1992, respectively; received Jan. 23, 1995; revision received Sept. 28, 1995; accepted for publication Oct. 2, 1995.

*Associate Professor, Department of Aeronautics and Astronautics, Code AA/Ho. Senior Member AIAA.

†Graduate Student, Aeronautical Engineering, Captain, U.S. Marine Corps; currently Staff Engineer, Veda Inc., 300 Exploration, Lexington Park, MD 20653.

‡Graduate Student, Aeronautical Engineering, Captain, U.S. Marine Corps; currently Senior Engineer, H-60 Helicopter Program, NADEP Cherry Point, NC 28533-0021.

Introduction

PAST success with unmanned air vehicles (UAVs) in the Persian Gulf War indicates their usefulness in obtaining timely intelligence during modern military conflicts. The Pioneer remotely piloted vehicle (RPV) has served in fleet and ground operations since 1987. Pioneer air vehicles logged 1011 h during 307 flights in Operation Desert Storm (see Fig. 1). The U.S. Navy employed the units to hunt for mines, provide gunfire support, perform reconnaissance for SEAL teams, and search for missile and antiaircraft artillery sites. The U.S. Marines used the UAVs for near-real-time targeting in conjunction with attack aircraft, and the U.S. Army employed them for route reconnaissance for AH-64 helicopter pilots. Of the 26 aircraft suffering damage, half were repaired in the field and returned to combat service.[1]

Because of the particular differences in the procurement and evaluation of manned and unmanned aircraft, problems may be identified that have not been fully explored in the limited test-and-evaluation process. Concerns expressed by the UAV Office at the U.S. Naval Air Warfare Center, Weapons Division (NAWC-WD), Pt. Mugu, involved issues of limited lateral–directional control and degraded pitch response at the high gross weights encountered.[2,3] These concerns have in the past led to relatively flat and fast approaches during shipboard net recovery, resulting in minor vehicle damage. During Pioneer tests at the U.S. Naval Air Warfare Center, Weapons Division, China Lake, a restricted c.g. travel necessitated the addition of lead weights to the nose of the air vehicle upon the testing of a new, more powerful (and heavier) engine; in other tests, a question of the sideslip capabilities reduced the maximum allowable crosswind component upon landing to 10 kn.

Training for the Pioneer normally requires use of the limited number of available vehicles by technicians, mechanics, and pilots. To provide cost-effective training, the Target Simulation Lab at the Pt. Mugu facility was tasked to develop a computer simulation of the Pioneer. Further objectives were to integrate the simulation into the Ground Control Station for internal pilot training and to couple it with a wide-screen display for training of the external pilot. During a typical operation the internal pilot controls the air vehicle when out of visual range, while the external pilot launches and recovers the aircraft visually. Aerodynamic data were needed to provide the necessary stability-and-control derivatives for an accurate simulation.

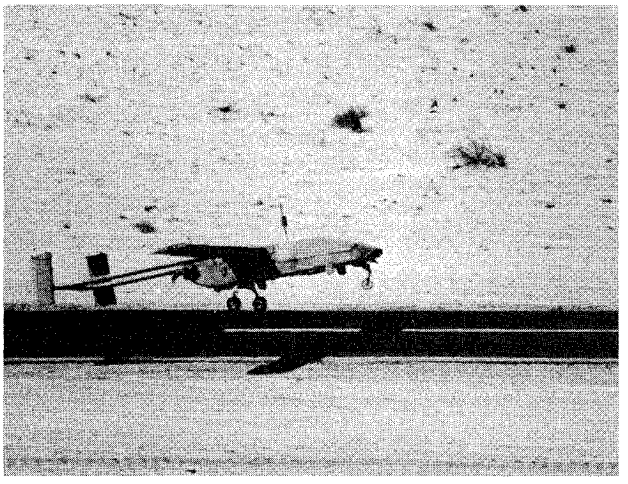

Fig. 1 Pioneer RPV.

A study was desired to quantify the air vehicle's static longitudinal and lateral–directional stability-and-control characteristics to answer important questions concerning the basic flying qualities of the Pioneer, as well as to complete the database of aerodynamic coefficients necessary to provide a computer-based simulation for training purposes. A multidirectional effort was conducted toward this goal, which included flight tests, wind-tunnel tests, and a computational analysis for performance and flying-qualities information. Comparisons between the different approaches will be presented; for a more complete description of the studies, see Refs. 4 and 5.

Experiments and Analysis

Flight Tests

A half-scale radio-controlled model of the Pioneer was used for the flight research investigation. Performance studies of the scaled air vehicle have been presented previously.[6] The radio-controlled aircraft weighed 35 lb, had a wingspan of 8 ft, and was of composite construction with aluminum tailbooms. The 0.91-ft-chord wing used the Clark-Y airfoil, with characteristics similar to those of the NACA 4415 airfoil used on the full-scale air vehicle. The tail on the flying model represents the early configuration, with the horizontal stabilizer spanning the width of the tailbooms (referred to as the small tail). The air vehicle was powered by a 25-cm^3 glow-fuel single-cylinder engine turning a custom 14-in. pusher propeller. The original radio-controlled model was designed for pilot training. Modifications made to the aircraft after being received from the manufacturer included the substitution of the new engine, the addition of flaps for better glide-path control and lower landing speeds, the movement rearward of the main landing gear for increased weight on the nosegear, and the substitution of a new nosegear using spring shocks with oil damping. Figure 2 shows the air vehicle before the addition of external instrumentation.

The aircraft was controlled using a standard nine-channel commercial hobby radio transmitter operating at 0.5 W in the 72-MHz band. A nose-boom instrumented with alpha and beta vanes turning small low-torque potentiometers was installed for measurement of angle of attack and sideslip angle. A pressure-transducer pitot–static system was used for indicated airspeed, with the pitot–static tube located 1.5 chords inboard of the right wingtip and projecting a chordlength ahead of the wing leading edge. Potentiometers linked by gearing to the controlling servomotors measured control-surface deflections.

Issues may be raised concerning accuracies of the air-data measurements. Normally in flight tests, an error-calibration procedure is followed to determine position-error corrections for the pitot–static system and the alpha–beta vanes. The usual methods could not easily be applied to the model aircraft.

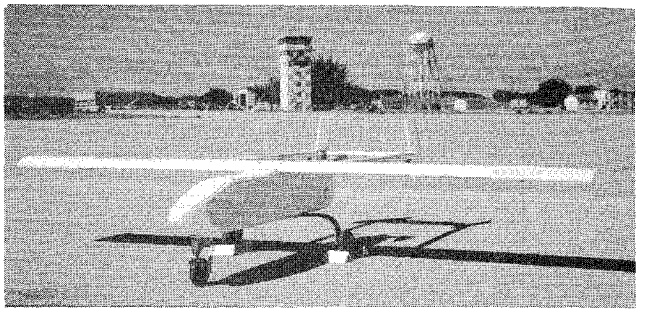

Fig. 2 One-half-scale Pioneer flight model.

Past studies[7,8] show the error induced in static pressure for a pitot–static probe mounted one chordlength in front of the wing leading edge near the wingtip to be about 1% of the flight dynamic pressure at the lift coefficients flown in the investigation. The corresponding error in airspeed would be on the order of 0.5%.[9] Errors for a probe located on a nose boom one fuselage diameter in front of the nose would generally be expected to be on the order of 4%. These errors incurred because of static-source position error are smaller than those expected from the measurements themselves, which are about 3% in airspeed[10] and 0.25–0.5 deg in angles of attack and sideslip.

A seven-channel telemetry system was designed and built to send the airborne data to a ground-based unit for recording and real-time display. Analog voltages from the airborne sensors were multiplexed, encoded, and downlinked as a single serial pulsewidth-modulated signal using a conventional radio-controlled rf deck operating at 0.6 W, sampling at 48 Hz, and transmitting in the 27-MHz band. The signal was received through a vertical antenna with ground plane at the receiver and was demultiplexed, decoded, and recorded by the portable unit mentioned earlier. The data were later digitized through an A/D board and personal computer.

Flight Test Procedure

Flights were performed at Fritzsche Army Airfield, Ft. Ord, California, and at a radio-controlled-model airfield at nearby Chualar, California. All flying was conducted within line of sight at altitudes below 400 ft. A typical flight lasted 10 min. A racetrack pattern was flown for the straight-and-level tests. Data were recorded for the aircraft once it was trimmed and steady during a 10-s window as it passed parallel to the runway. Display meters calibrated in appropriate units on the ground-unit panel displayed the flight data in real-time, and an event marker manually input at the ground unit would designate the point on the recorded tape at which desired data were to be observed. Calibrations (voltage outputs for known inputs) of all control-surface deflections, the alpha–beta vanes, and the pressure transducer were performed at the field before each flight.

Static Longitudinal Tests

A lack of knowledge of controllability and flight characteristics at low speeds restricted the allowable c.g. travel for the full-scale Pioneer UAV. Net recoveries were made with relatively fast and flat approaches, often resulting in minor damage, such as broken propellers or antennas. A determination was needed of the aircraft's neutral point to ascertain if the c.g. range could be expanded. The nominal c.g. position of the half- and full-scale vehicles was designated as 33% mean aerodynamic chord (mac).

Longitudinal tests consisted of trimmed level flights at different airspeeds and c.g. positions. Each flight consisted of six passes at a different speed. Airspeeds varied from 36 to 68 knots indicated airspeed (KIAS). Center-of-gravity positions were 32.3% mac for the first flight, 30.9% for the second, and 36.7% for the third. Wind gusts and aft-c.g. sensitivity on the approach of the final flight resulted in a hard landing that dam-

aged the right wing. Later, the third set of data was found to be unusable because of unreliable airspeed information. Results are shown using the first two data sets.

Static Lateral–Directional Tests

The steady-heading sideslip maneuver was performed for various sideslip angles for the determination of rudder and aileron response to sideslip and bank angle for the trimmed aircraft. Of interest was whether the rudder or aileron provided the limiting factor in the sideslip and what the actual value of the sideslip and crosswind limit was. Runs were made at a c.g. of 33.4% mac at speeds between 55–70 KIAS. Passes consisted of steady flybys with the application of rudder and with the use of aileron to maintain a straight track on a constant heading. Application for the five test points were half rudder, full rudder, no rudder, and then the same in the opposite direction. Plots of rudder and aileron deflection required to maintain a measured sideslip angle provide a determination of the maximum limit of sideslip angle, or crosswind for a desired ground tracking, as during the landing approach. Maximum deflections for all three control surfaces of the full-scale Pioneer are ±20 deg.

Wind-Tunnel Tests

Wind tunnel tests were conducted of a 0.4-scale model of the Pioneer RPV (Fig. 3) in the Wichita State University 7 by 10 ft wind tunnel at a full-scale Reynolds number of 1×10^6. The aircraft is a twin-boom pusher configuration. The wing and tail surfaces were milled from solid aluminum and had moving control surfaces. The remainder of the airframe was constructed of steel, aluminum, wood, and composites. Powered tests were carried out using a water-cooled variable-speed electric motor and variable-pitch propeller, but no powered data will be presented here. The airfoil used was the NACA 4415 section as on the full-scale vehicle. Vertical and horizontal stabilizers used the NACA 0012 airfoil section. The tail section used on the wind-tunnel model was the new configuration, consisting of a tail span increased beyond the tailboom width for an area 75% greater than that of the original tail. Results of tests with the two different tails will be noted where appropriate.

The wind tunnel is a closed-circuit unpressurized facility with the ambient turbulence characterized by a turbulence factor of 1.13 at the test dynamic pressure of 50 psf. An external six-component truncated pyramidal balance was used for the measurements. At the test q, resolution of C_L was 0.0008, C_D was 0.0002, and C_m was 0.0001. Buoyancy, blockage, and tare-and-interference corrections were applied (see Ref. 11 for a more complete discussion).

Tests were conducted to gather data for the determination of drag and power required, elevator and rudder power, aileron effectiveness, pitch stability, weathercock stability, dihedral effect, and crosswind capability. Values that can be compared to those from the other tests will be included here.

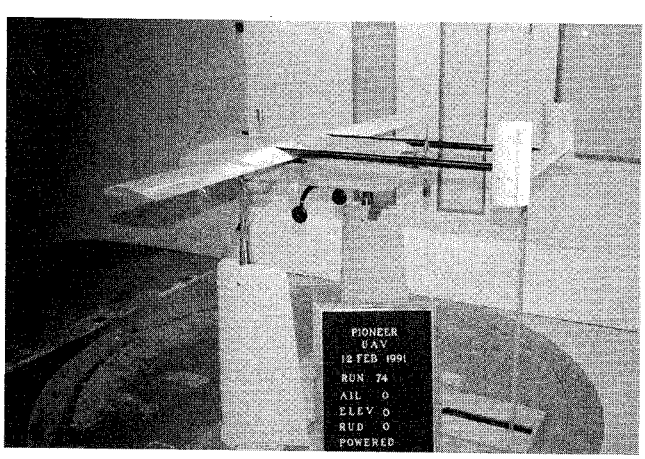

Fig. 3 Four-tenths-scale Pioneer wind-tunnel model.

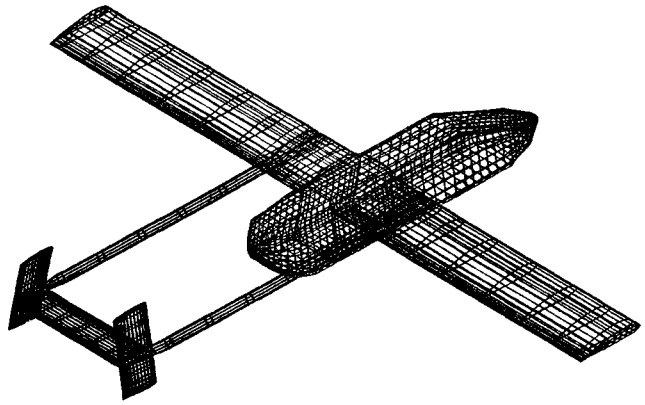

Fig. 4 Pioneer computer panel-code model.

Numerical Analysis

A third program involved the application of a nonproprietary version of a low-order panel code, VSAERO, to the Pioneer aerodynamic analysis. In this code developed at the NASA Ames Research Center, PMARC, a distribution of source and doublet singularities is placed on quadrilateral panels of the air-vehicle surface geometry (see Fig. 4). The singularities are constant over each panel, leading to the lower-order method. Varying singularities lead to greater accuracy, but also to greater complexity and computational time. The doublet strengths on the surface panels are calculated iteratively to solve for a solution yielding tangential flow over the panels. The computer program allows for the application of a time-stepping wake that satisfies the Kutta condition at the wing trailing edge.

The version of the code used limited the panel distribution to 5000 panels. Because of symmetry, only the half-plane was modeled for the longitudinal study. Use of 3000 panels on the half-plane model precluded the complete model from being tested in the directional study. The directional stability-and-control analysis was carried out using the combined effects of the components (wing, tail, and fuselage) with no accommodation for sidewash. Data from the numerical analysis will be compared to the results of the other tests to demonstrate their validity and limitations.

Results

Longitudinal

In the flight tests, two data points were taken on each pass. Known limitations of the tape playback unit used in the digitizing process required the smoothing of data sampled at a high rate; data were read at 5 kHz for 0.25 s and averaged for a single data point. Plots of elevator deflection vs lift coefficient provided a series of slopes that were extrapolated to find the aircraft stick-fixed neutral point.[12] Figures 5 and 6 show the plots at the forward and nominal c.g. locations. Data scatter are higher than desired, but are as expected in radio-controlled testing where conditions are maintained visually. Extrapolation of the elevator deflection with C_L results in the c.g. location where no deflection change is required to retrim the aircraft, i.e., the neutral point. Because radio-controlled aircraft are fly-by-wire, the neutral point is stick-fixed, and stick-free criteria do not apply.

A value of 47.7% mac is given by the plot in Fig. 7. The amount of extrapolation is greater than preferred, but the failure of the air–data system on the aft-c.g. flight precluded use of those data. Further testing is required before any reasonable level of confidence can be placed on the flight results for this case and the results must be considered to be preliminary.

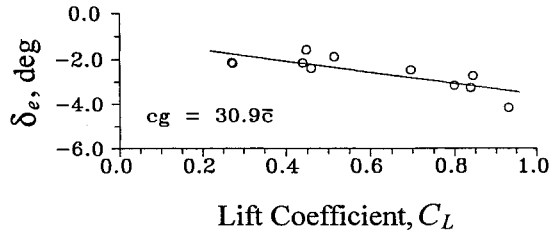

Fig. 5 Elevator deflection vs lift coefficient to trim, 30.9% mac.

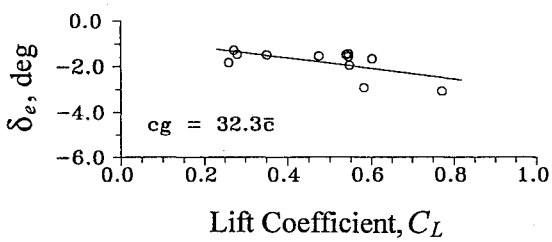

Fig. 6 Elevator deflection vs lift coefficient to trim, 32.3% mac.

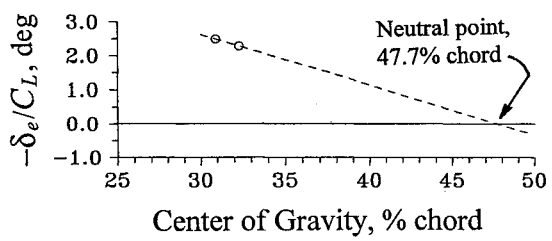

Fig. 7 Neutral point determination.

A comparison of the flight results (with the small tail) can be made to classical theory[13] and to the computer panel-code predictions; for the large tail, comparisons can be made between the results of the wind-tunnel tests and the panel-code predictions. In the theoretical approach, the neutral point can be estimated from the aircraft geometry and the lift-curve slopes of the wing and tail. An estimated neutral-point location for the half-scale Pioneer based on the configuration was 47%.[14] The panel code resulted in a prediction of the neutral point of 51%. The flight and computer results are plotted in Fig. 8 for the small tail, along with wind-tunnel and computer results for the large tail. No flights were performed with a large tail, and no wind-tunnel tests were conducted with a small tail.

In the wind-tunnel tests, the moment reference center is easily translated to treat various c.g. locations. Taking the moments at various locations and extrapolating $C_{m\alpha}$ to zero at the various lift coefficients produces the stick-fixed neutral-point location as a function of C_L. While the panel code and flight-test results were close for the small tail, the panel code and wind-tunnel results are off by 10% mac over much of the angle-of-attack regime for the large tail. As flow separation starts to take place on the wind-tunnel model, the actual neutral point moves aft as shown in the figure. Of course, linear theory cannot predict this movement. From observation of the small-tail data, it does appear that a scaled radio-controlled model is sufficient to accurately predict the static longitudinal behavior of the Pioneer UAV.

It should be stressed that the air vehicle simulated by the half-scale flying model possessed a small tail, representing the early configuration. The current Pioneer is flying with a tail area increased by 75% (as tested in the wind tunnel) to alleviate potential longitudinal stability-and-control problems. The c.g. range specified for the early Pioneer was probably required for reasonable longitudinal control under normal flight operations. The static margin indicated by the flight-model test results of 14–15% appears reasonable from a stability viewpoint, and should warrant no concern. However, the small

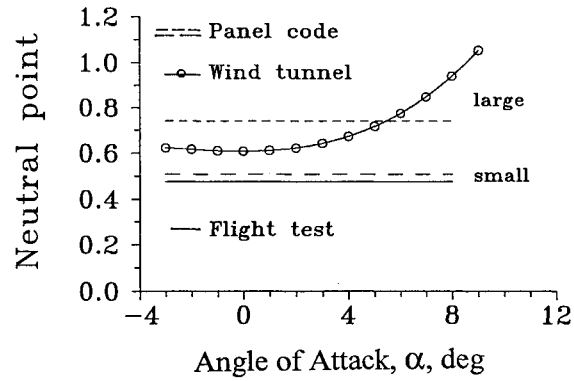

Fig. 8 Neutral point comparison: flight test and panel code, small tail; wind tunnel and panel code, large tail.

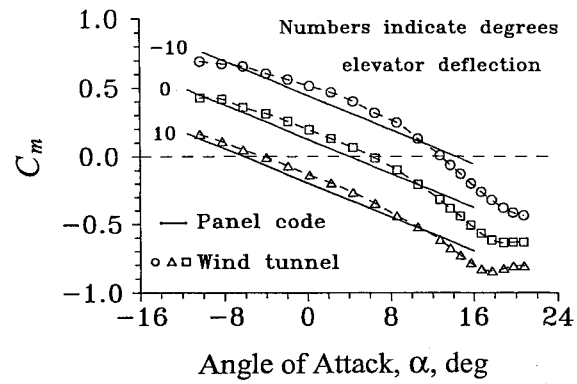

Fig. 9 Pitching moment coefficient vs angle of attack for three elevator deflections, wind tunnel and panel code.

elevator chord, together with the immersion of the tail in the reduced dynamic pressure of the propeller slipstream upon power reductions (such as during the approach phase), suggested an improvement in the controllability of the vehicle at low speeds.

Plots of C_m vs α for three elevator deflections are shown in Fig. 9 for the large-tail configuration. Compared are the wind-tunnel and computer-simulation data. The data are referenced to the 33% mac c.g. position, the nominal one for this aircraft. The experimental slopes are α dependent, though well-behaved over the expected flight regime. The elevator control power $C_{m\delta e}$ is evident from the shift between the curves with elevator deflections. Though the experimental and numerical plots are shifted slightly in the trim regime of 4- to 6-deg angle of attack, the slopes are very similar, as are the amounts of the shifts with the application of elevator. No flights were possible with a large tail because there were none being built by the manufacturer of the half-scale model. (A comparison of values for elevator control power is shown in Fig. 10.)

Static margins appear to be sufficient for both small- and large-tail configurations, from a stability consideration. Values of $C_{m\alpha}$ and $C_{m\delta e}$ for the large-tail version match fairly well with those of a twin-engine commuter aircraft,[15] indicating the adequacy of the improved tail from a static longitudinal stability-and-control viewpoint. Longitudinal derivatives derived from wind-tunnel tests and panel-code simulation, along with those supplied by the Pioneer manufacturer,[16] are shown in Table 1. Agreement is good between the tested data, but discrepancies exist when compared to provided data.

Lateral–Directional

Results of the test flights are compared to other test data. The wind-tunnel test resulted in values of rudder deflection to maintain sideslip angle. The computer model predicted sideslip

Table 1 Pioneer longitudinal stability and control derivatives[a]

Derivative	Wind tunnel	Panel code	Manufacturer
$C_{L\alpha}$	4.78	4.39	5.01
$C_{m\alpha}$	−2.12	−1.80	−0.690
$C_{L\delta e}$	0.401	0.407	0.17
$C_{m\delta e}$	−1.760	−1.833	−0.75

[a]All derivatives are per radian.

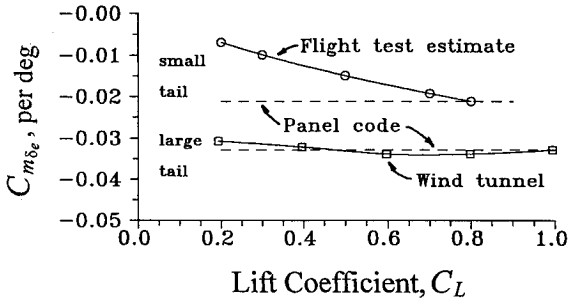

Fig. 10 Elevator control power vs lift coefficient: flight test and panel code, small tail; wind tunnel and panel code, large tail.

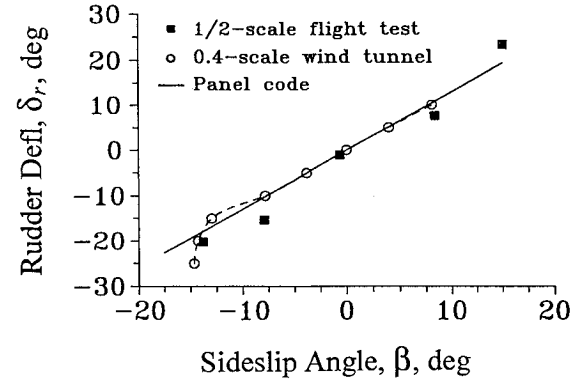

Fig. 11 Rudder deflection vs sideslip angle, trimmed sideslips.

trim requirements and data provided by the Pioneer manufacturer were used to extract similar data.

In a steady sideslip, deflections of rudder and aileron are required to maintain the desired sideslip and bank angles. The horizontal component of the tilted lift vector is required to balance the generated side force, while the sums of the yawing and rolling moments are zero. The relations for side force, yawing moment, and rolling moment are

$$C_{Y\beta}\cdot\beta + C_{Y\delta r}\cdot\delta_r + C_{Y\delta a}\cdot\delta_a = -C_L\cdot\sin(\phi) \quad (1)$$

$$C_{n\beta}\cdot\beta + C_{n\delta r}\cdot\delta_r + C_{n\delta a}\cdot\delta_a = 0 \quad (2)$$

$$C_{l\beta}\cdot\beta + C_{l\delta r}\cdot\delta_r + C_{l\delta a}\cdot\delta_a = 0 \quad (3)$$

This maneuver, though easy to establish in flight, is difficult and unnecessary to set up in a wind-tunnel situation. Once the stability-and-control derivatives in the previous equations are determined individually for a given lift coefficient, the bank angle can be varied, and values of β, δ_r, and δ_a can be determined from the set of equations. This process was followed with the wind-tunnel data and those supplied by the manufacturer.

Figure 11 shows the required rudder deflection per sideslip angle for the three cases. The circles represent the wind-tunnel results. The response is linear from 10 to −10 deg of rudder input, until the rudder begins to stall at around 15 deg. Further application of rudder is mostly ineffective, up to the maximum input of 25 deg. The solid line from the computational study

Table 2 Sideslip results

Ratio	Flight test	Wind tunnel	Panel code
δ_r/β	1.48	1.25	1.29
δ_a/β	0.18	0.16	——
δ_a/δ_r	0.124	0.127	——

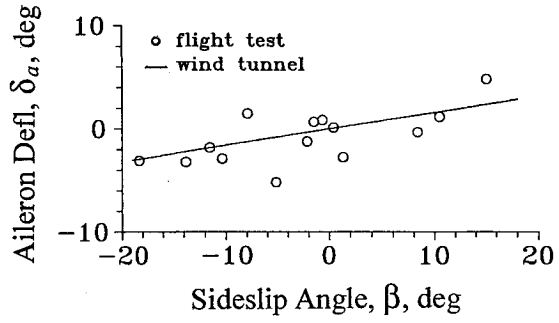

Fig. 12 Aileron deflection vs sideslip angle, trimmed sideslips.

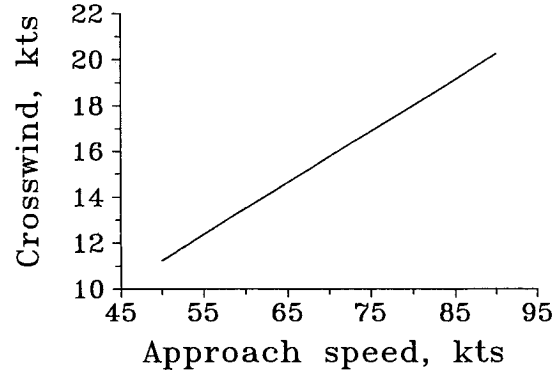

Fig. 13 Crosswind limits based on available rudder power.

matches the wind-tunnel results perfectly throughout the linear region. The panel-code does not account for viscosity and therefore cannot predict any stalled behavior. The black squares represent the flight points from 22 to −22 deg of rudder input. The points follow the previous two plots fairly well, with a sideslip of about 14 deg resulting from a 22-deg rudder input. Scatter is evident, but the slope of the data matches the others reasonably well.

Figure 12 shows the comparison of flight-test results with those of the wind-tunnel tests for the required aileron deflection during the steady sideslip maneuvers. The flight data (circles) represent the results of a number of separate flights. Though the scatter is large, the scaled flight test and the wind-tunnel results can be seen to match very well, with only a few deg of aileron being required to maintain the sideslip condition.

The manufacturer's supplied data provided values that disagreed widely with the other results. As calculated, the results implied that the sideslip angle was greater than the required rudder input, and that twice the aileron deflection noted was required. Such apparent discrepancies are possible and not easily discovered in a long list of stability-and-control derivatives provided to the end user. Should full-scale flight data become available, these results can be checked to verify the measured values and to further explore the noted discrepancies.

The sideslip results can be summed up in a listing of the ratios of δ_r to β, δ_a to β, and δ_a to δ_r, as shown in Table 2. Again, it can be seen that the general agreement between the half-scale flight results, the wind-tunnel results, and the panel-code results indicate the usefulness of using scaled radio-controlled aircraft for the determination of static stability-and-control derivatives for simulation or training. As a side note, the

scaled flight test is estimated to cost a fraction of commercial wind-tunnel tests or full-scale flight tests.

A crosswind capability is defined as the ability to track a heading (the runway centerline) in a crosswind; it involves the ability of the rudder to induce a sideslip. Though aileron deflection required to counter the rolling moment also induces an adverse yaw, the tendency to roll is extremely small for the Pioneer, and the aileron input was neglected in this analysis. Based on the rudder limit of 15 deg to maintain a 13-deg sideslip, a plot of limiting direct crosswind vs approach speed can be given, as shown in Fig. 13. It is recommended, for example, that 14-kn crosswinds be approached at speeds no less than 65 kn.

Conclusions

Longitudinal flight tests, supported by wind-tunnel tests and computer simulation, indicate that the static margin of the Pioneer should be sufficient for the c.g. envelope to be opened. However, control limitations because of the small elevator and propwash effects may be the deciding factor for tail size. For the half-scale flight model, significant pitch changes on approach because of power changes lead to the addition of flaps for improved flight-path control. With flaps, power was able to be maintained while approach speeds were reduced. The maintenance of power caused the dynamic pressure seen by the tail to remain high, resulting in more consistent approaches and fewer trim changes.

Lateral–directional tests indicate the limiting control surface to be the rudder when compensating for crosswind conditions. Rudder stall begins at about 15 deg, resulting in 13 deg of sideslip. Crosswind limits should be placed on operations accordingly.

Comparisons of the half-scale tests with wind-tunnel and computational results indicate the benefits of radio-controlled flight testing, in particular with unknown or unproven configurations. Identified problems can be explored and studied and recommendations made at low cost in work-hours and equipment investment.

Acknowledgments

The first author wishes to thank the UAV lab technician and pilot Don Meeks for his piloting and fabrication skills. This work was performed in part for the NAWC-WD Pt. Mugu, and for the Unmanned Air Vehicle Joint Project, Washington, D.C. The first and second authors thank Keith Bratberg and Steve Dean at NAWC-WD Pt. Mugu for their support during the wind-tunnel tests. Funding for the radio-controlled flight program was provided by the U.S. Naval Postgraduate School, for which the first author is grateful. The first author also thanks the students involved with the various parts of the radio-controlled flight-test program: Jim Salmons, Kent Aitcheson, Kevin Wilhelm, and Paul Koch.

References

[1]"Gulf War Experience Sparks Review of RPV Priorities," *Aviation Week and Space Technology*, April 22, 1991, p. 86.

[2]"Pioneer Short Range Remotely Piloted Vehicle Flight Test Based Aerodynamic and Engine Performance," Fleet Combat Systems Lab., Pacific Missile Test Center, Point Mugu, CA, Dec. 1987.

[3]"Initial Report for Contractor Development Tests on Baseline Pioneer and Associated Modifications," Unmanned Air Vehicle Office, Pacific Missile Test Center, Point Mugu, CA, Dec. 1988.

[4]Howard, R. M., and Bray, R. M., "Flight Test and Wind-Tunnel Study of a Scaled Unmanned Air Vehicle," AIAA Paper 92-4075, Aug. 1992.

[5]Bray, R. M., Lyons, D. F., and Howard, R. M., "Aerodynamic Analysis of the Pioneer Unmanned Air Vehicle," AIAA Paper 92-4635, Aug. 1992.

[6]Howard, R. M., Tanner, J. C., and Lyons, D. F., "Flight Test of a Half-Scale Unmanned Air Vehicle," *Journal of Aircraft*, Vol. 28, No. 12, 1991, pp. 843–848.

[7]Perkins, C. D. (ed.), *Flight Test Manual Vol. I Performance*, AGARD, Pergamon, New York, 1959, pp. 1:17–1:35.

[8]Gracey, W., "Measurement of Aircraft Speed and Altitude," NASA RP-1046, June 1980, pp. 77, 95.

[9]Schenck, H., Jr., *Theories of Engineering Experimentation*, McGraw–Hill, New York, 1961, pp. 46, 47.

[10]"Model 1221D Mini Indicated Airspeed Transducer," Product Data Sheet 2228, Rosemount Inc., Burnsville, MN, 1983.

[11]Bray, R. M., "A Wind Tunnel Study of the Pioneer Remotely Piloted Vehicle," Masters Thesis, Naval Postgraduate School, Monterey, CA, June 1991.

[12]Perkins, C. D. (ed.), *Flight Test Manual Vol. II Stability and Control*, AGARD, Pergamon, New York, 1959, pp. 3:7–3:10.

[13]Anderson, J. D., Jr., *Introduction to Flight*, McGraw–Hill, New York, 1989, pp. 383–388.

[14]Aitcheson, K. R., "Stability and Control Flight Testing of a Half-Scale Pioneer Remotely Piloted Vehicle," Masters Thesis, Naval Postgraduate School, Monterey, CA, Sept. 1991, p. 41.

[15]Roskam, J., *Airplane Flight Dynamics and Automatic Controls*, Roskam Aviation and Engineering, Ottawa, KS, 1982, pp. 598–600.

[16]Correspondence from Al Ellis, AAI Corp., to James Salmons, Sept. 11, 1990.